Supporting Information

Earth Abundant Fe/Mn-Based Layered Oxide Interconnected Nanowires for Advanced K-Ion Full Batteries

Xuanpeng Wang, Xiaoming Xu, Chaojiang Niu*, Jiashen Meng, Meng Huang, Xiong Liu, Ziang Liu, Liqiang Mai*

State Key Laboratory of Advanced Technology for Materials Synthesis and Processing, Wuhan University of Technology, Wuhan 430070, China

Email: mlq518@whut.edu.cn; niuchaojiang11@whut.edu.cn

Key words: Interconnected nanowires, K-ion full batteries, Fe/Mn-based layered oxide, high-capacity, superior cycling stability, *in situ* X-ray diffraction

EXPERIMENTS

Synthesis of Interconnected $K_{0.7}Fe_{0.5}Mn_{0.5}O_2$ Nanowires and $K_{0.7}Fe_{0.5}Mn_{0.5}O_2$ Particles

The polyvinylpyrrolidone (PVP) (4.0 g, K-30, M_w=40000), CH_3COOK (3.5 mmol), iron(III) acetylacetonate (2.5 mmol) and manganese(II) Acetyllacetonate (2.5 mmol) were mixed in deionized water (40 mL) at 25 °C for 8 h. When the solution was obtained, it was then delivered into a metallic needle at a constant flow rate of 0.4 mL h^{-1}, and the nanowiress were obtained through electrospinning method with a high voltage of 21.0 kV. The obtained product was then sintered at 300 °C in air for 2 h (2 °C min^{-1}), and sintered at 800 °C in argon for 8 h (5 °C min^{-1}) to obtain interconnected $K_{0.7}Fe_{0.5}Mn_{0.5}O_2$ nanowires. As control experiments, the $K_{0.7}Fe_{0.5}Mn_{0.5}O_2$ particles were obtained by directly sintering in the same condition, without electrospinning. Soft carbon was prepared by pyrolysis PTCDA (Perylene-3,4,9,10-tetracarboxylic dianhydride) in a tube furnace at 900 °C for 10 h (4 °C min^{-1}) under argon atmosphere. [17]

Material Characterization

In situ X-ray diffraction (XRD) experiment during electrochemical testing of battery was performed on a Bruker D8 Discover X-ray diffractometer with a non-monochromated Cu Kα X-ray source scanned at 2θ ranges of 17.0–46.0°. For *in situ* XRD measurement, the electrode was placed right behind an X-ray-transparent beryllium window which also acts as a current collector. The *in situ* XRD signals were collected using the planar detector in a still mode during the charge/discharge processes, and each pattern took 200 s to acquire. Cathodes were obtained with 70% active material, 20% acetylene black and 10% PVDF (using N-methyl-2-pyrrolidone solvent by weight). The reference electrode was K metal (99.5%, Sigma-Aldrich). A 0.8 M KPF_6 solution in a mixed solvent of ethylene carbon/dimethyl carbonate (1:1 w/w) was used as the electrolyte; a whatman glass microfiber filter paper (grade GF/F) was used as the separator.

The cathode was cut into square slices with an area of ~0.49 cm^2 and a thickness of ~0.1 mm. The loading mass of the active material was approximately 1.4–1.6 mg cm^{-2}.

Powder XRD measurements were performed to obtain the crystallographic information using a Bruker D8 Discover X-ray diffractometer equipped with a non-monochromated Cu Kα X-ray source. Field-emission scanning electron microscopy (FESEM) images were collected using a JEOL-7100F microscope. Energy-dispersive X-ray spectroscopy (EDS) was performed using an Oxford EDS IE250. Transmission electron microscopy (TEM) and high-resolution TEM was conducted on a JEOL JEM-2100F STEM/EDS microscopy. TG-DSC was performed on a STA-449C. Raman spectra were obtained using a Renishaw INVIA micro-Raman spectroscopy system.

Electrochemical Measurements

The electrochemical measurements were carried out by using 2016 coin cells, which were assembled in a glove box filled with pure argon gas, and used K metal (99.5%, Sigma-Aldrich) as the reference electrode, A 0.8 M KPF_6 in a mixture of ethylene carbon/dimethyl carbonate (1:1 w/w) as electrolyte; a whatman glass microfiber filter (Grade GF/F) as the separator. Cathodes were composed of 70% active material, 20% acetylene black, and 10% PVDF (using N-methyl-2-pyrrolidone as a solvent) in weight. The cathodes and anodes were cut into square slice with ~0.49 cm^2 in area and ~0.1 mm in thickness. The loading of cathode and anode materials are approximately 1.4–1.6 mg cm^{-2} and 1.8–2.0 mg cm^{-2}, respectively. Before assembly full cell, the soft carbon electrode and metal potassium were putted together directly, and 4-6 drops electrolyte was covered on the soft carbon electrode plate, keeping 60-70 seconds in an argon-gas-filled glove box. Galvanostatic charge/discharge tests of cathode and anode were performed at potential range from 1.5 to 4.0 V and from 0.01 to 1.5 V *vs.* K^+/K using a multichannel battery testing system (LAND CT2001A), respectively. The GITT test for interconnected $K_{0.7}Fe_{0.5}Mn_{0.5}O_2$ nanowires at a current density of 6.7 mA g^{-1} using a multichannel battery testing system (LAND CT2001A). The full cells were performed at a potential range of 0.5–3.5 V *vs.* K^+/K using a multichannel battery testing system (LAND CT2001A). Cyclic voltammetry (CV) and electrochemical impedance spectra (EIS) were conducted using an electrochemical workstation (CHI600E and Autolab PGSTAT 302N).

Calculation of the K-ion Diffusion Kinetics

$$I_p = 0.4463nFAC\left(\frac{NFvD}{RT}\right)^{1/2} = [269000 \times n^{3/2}ACD]v^{1/2} \quad (1)$$

Here I_p is the peak current, n is the number of electrons transferred per molecule during the electrochemical reaction (here 1), A is the active surface area of the electrode (here $3.752\times\pi$ mm^2), C is the concentration of K-ions in the cathode (here 1), D is the apparent K-ions diffusion coefficient of the whole electrode involving the diffusion of both K-ions and electrons, and v is the scanning rate.

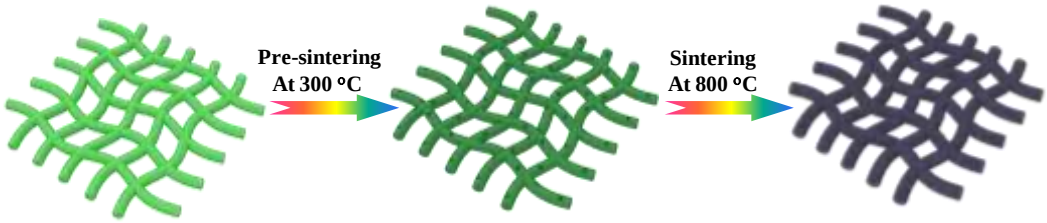

Figure S1. Schematic illustration of interconnected $K_{0.7}Fe_{0.5}Mn_{0.5}O_2$ nanowires formation.

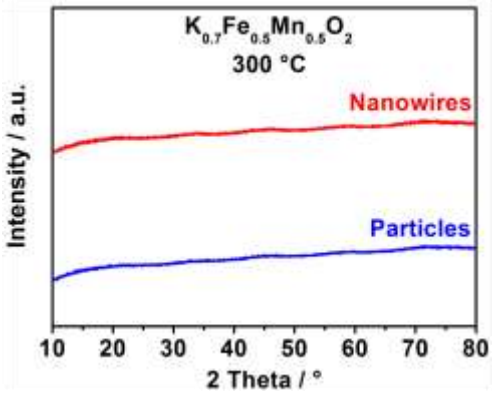

Figure S2. XRD patterns of the precursor of interconnected $K_{0.7}Fe_{0.5}Mn_{0.5}O_2$ nanowires and $K_{0.7}Fe_{0.5}Mn_{0.5}O_2$ particles presintered at 300 °C.

Table 1. ICP test results of interconnected $K_{0.7}Fe_{0.5}Mn_{0.5}O_2$ nanowires and $K_{0.7}Fe_{0.5}Mn_{0.5}O_2$ particles sintered at 800 °C, respectively.

$K_{0.7}Fe_{0.5}Mn_{0.5}O_2$	**K:Fe:Mn**
Interconnected Nanowires	0.700:0.496:0.501
Particles	0.700:0.498:0.496

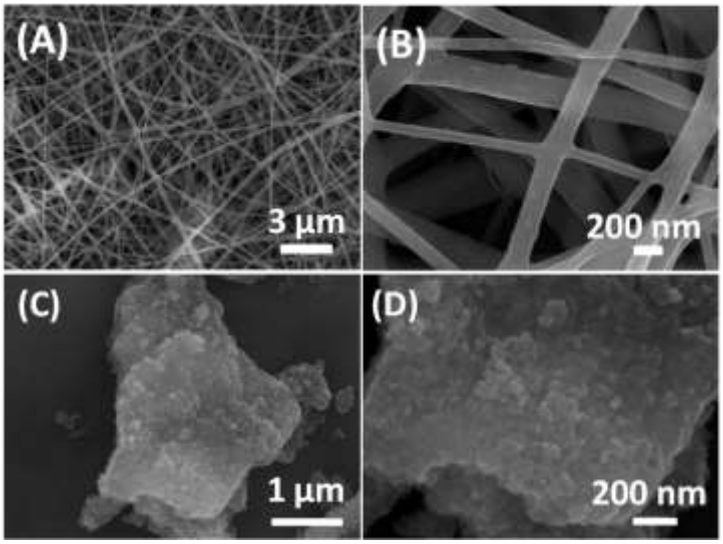

Figure S3. (A, B) SEM images of the interconnected $K_{0.7}Fe_{0.5}Mn_{0.5}O_2$ nanowires presintered at 300 °C. (C, D) SEM images of $K_{0.7}Fe_{0.5}Mn_{0.5}O_2$ particles pre-sintered at 300 °C.

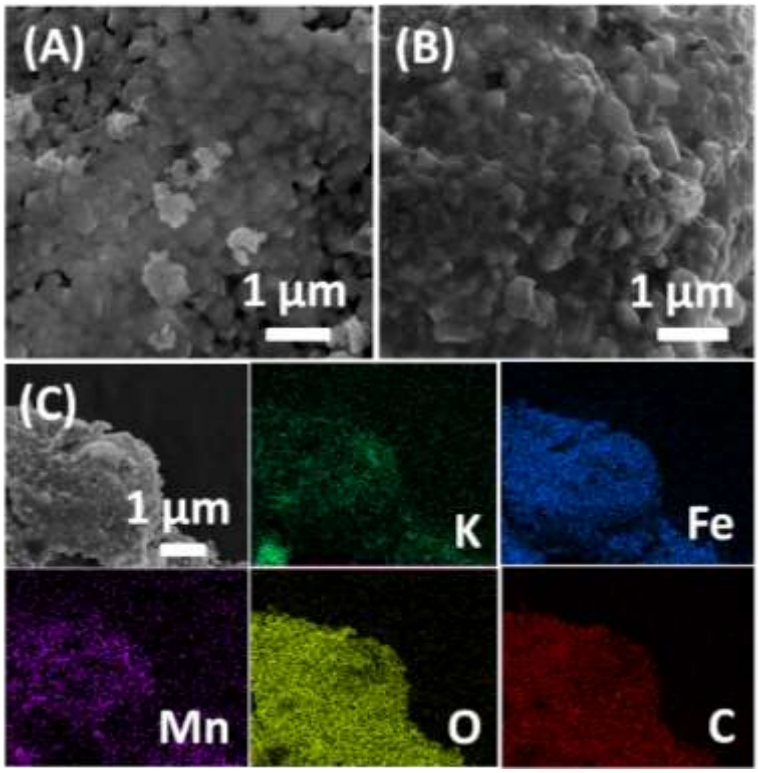

Figure S4. SEM images (A, B) and EDS mapping (C) of $K_{0.7}Fe_{0.5}Mn_{0.5}O_2$ particles sintered at 800 °C.

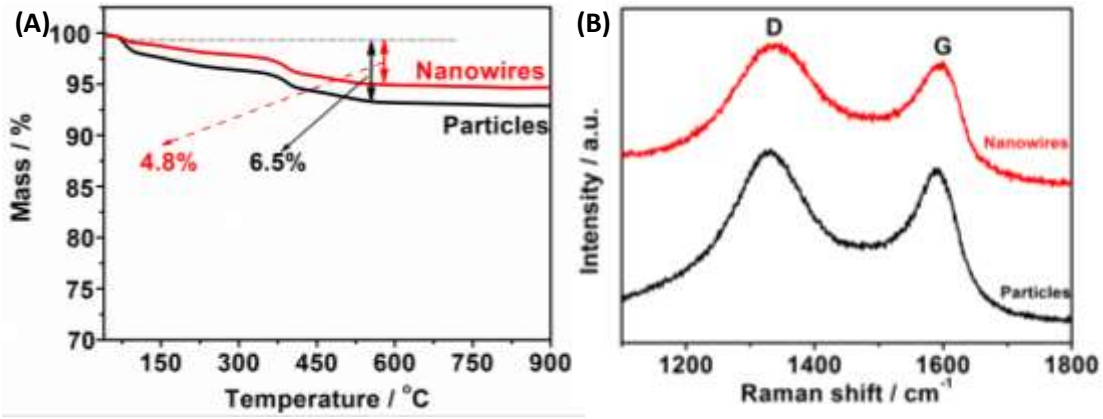

Figure S5. (A) TGA curves and Raman spectra (B) of interconnected $K_{0.7}Fe_{0.5}Mn_{0.5}O_2$ nanowires and $K_{0.7}Fe_{0.5}Mn_{0.5}O_2$ particles sintered at 800 °C, respectively.

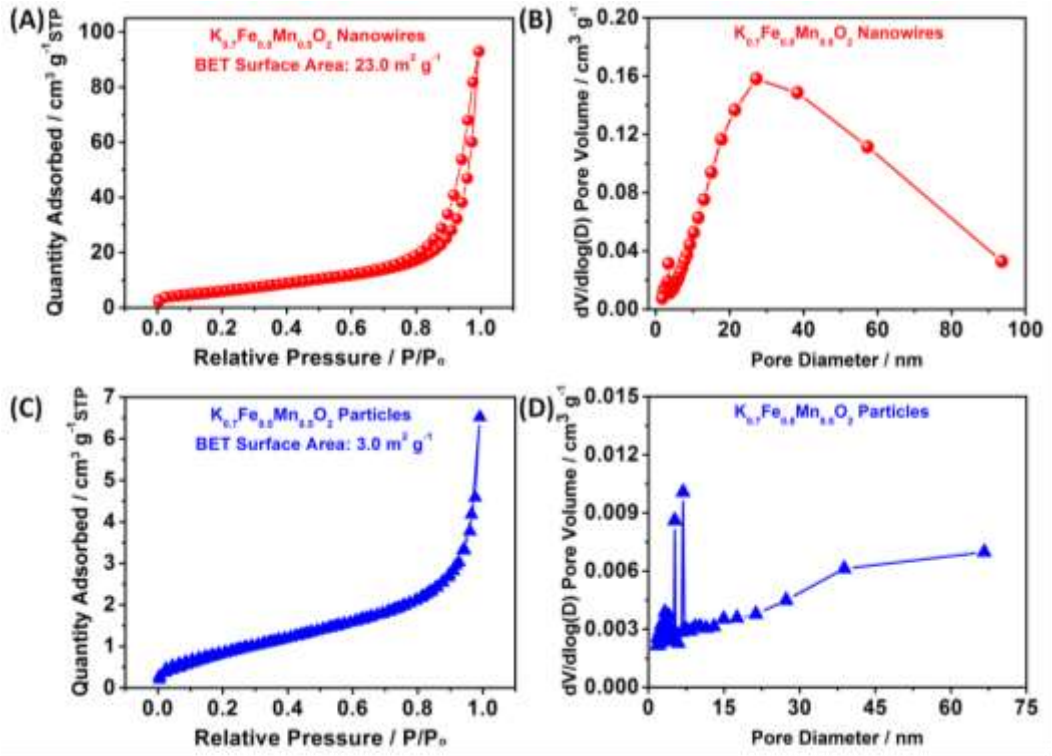

Figure S6. The nitrogen adsorption-desorption isotherms (A) and pore size distribution (B) of the interconnected $K_{0.7}Fe_{0.5}Mn_{0.5}O_2$ nanowires. The nitrogen adsorption-desorption isotherms (C) and pore size distribution (D) of the $K_{0.7}Fe_{0.5}Mn_{0.5}O_2$ particles.

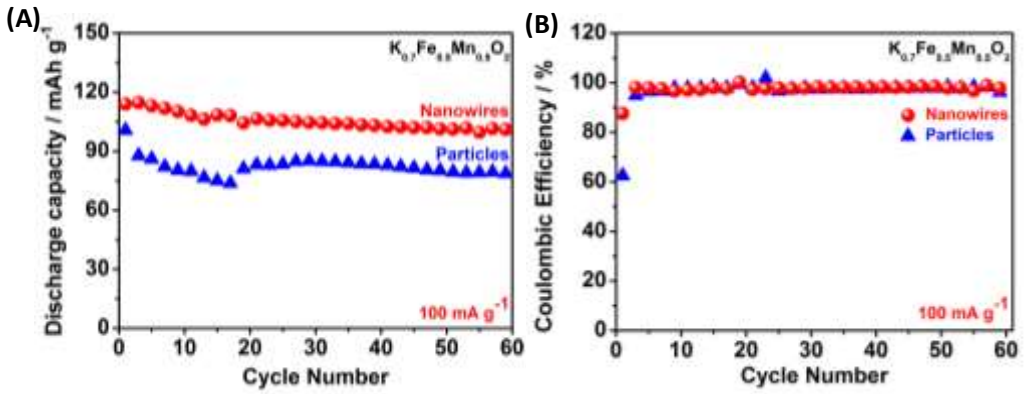

Figure S7. Cycling performance (A) and corresponding Coulombic efficiency (B) of interconnected $K_{0.7}Fe_{0.5}Mn_{0.5}O_2$ nanowires and $K_{0.7}Fe_{0.5}Mn_{0.5}O_2$ particles at 100 mA g^{-1}, respectively.

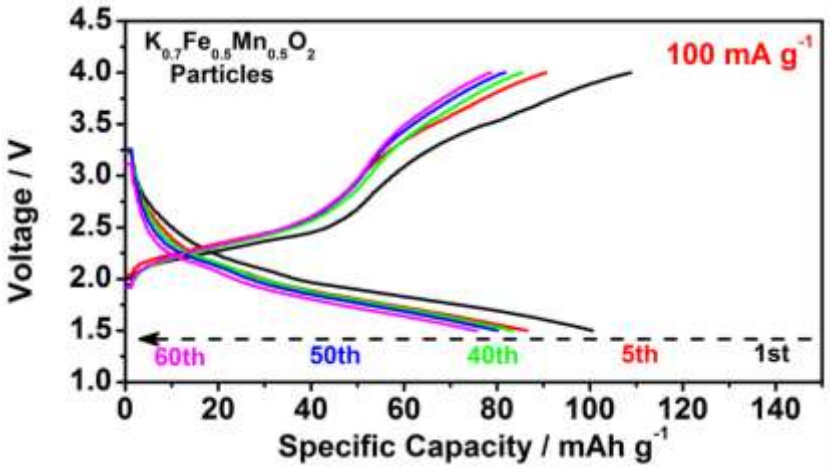

Figure S8. Charge-discharge curves of $K_{0.7}Fe_{0.5}Mn_{0.5}O_2$ particles at 100 mA g^{-1}.

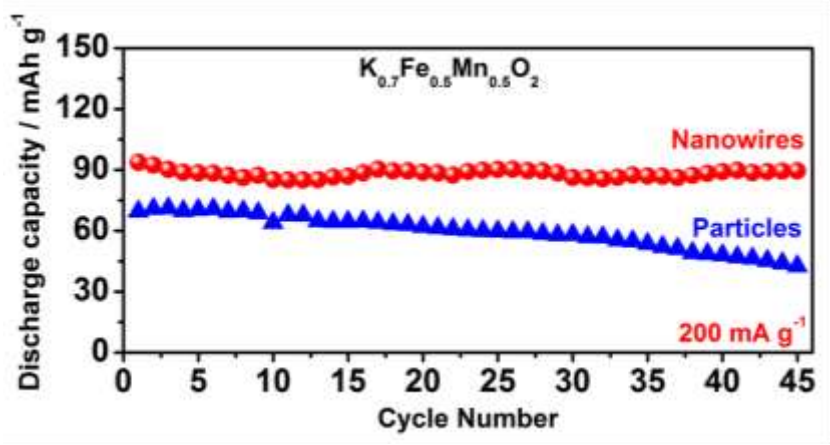

Figure S9. Cyclic performance of interconnected $K_{0.7}Fe_{0.5}Mn_{0.5}O_2$ nanowires and $K_{0.7}Fe_{0.5}Mn_{0.5}O_2$ particles at 200 mA g^{-1}.

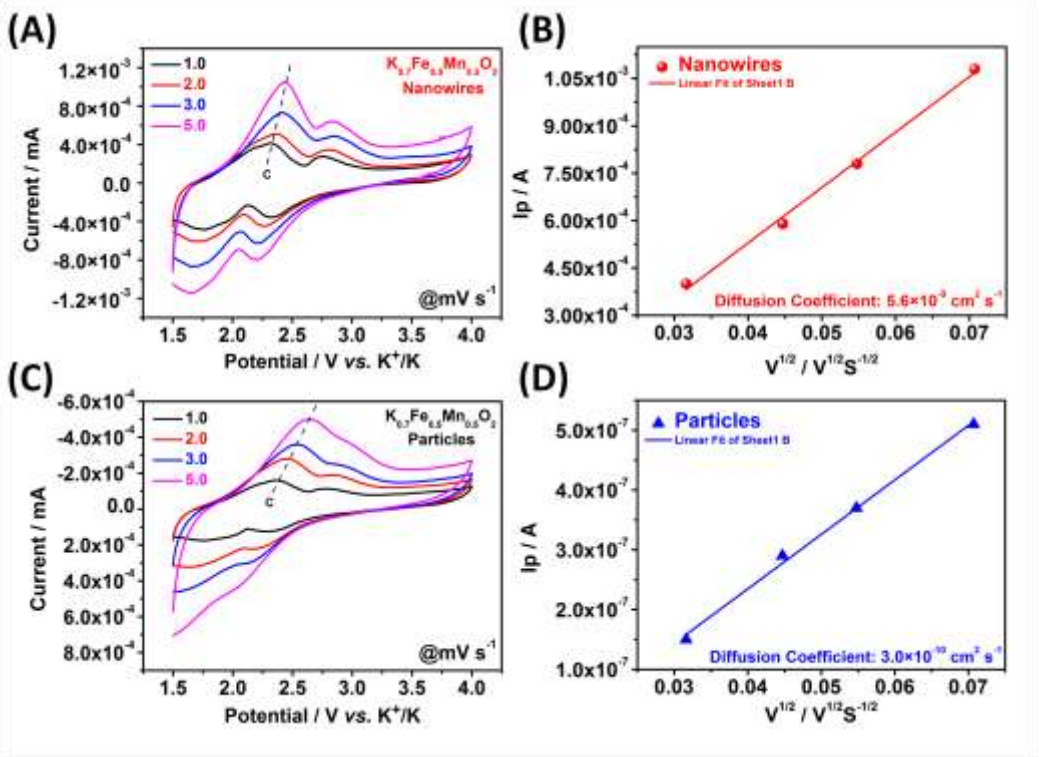

Figure S10. (A) CV curves of interconnected $K_{0.7}Fe_{0.5}Mn_{0.5}O_2$ nanowires in the electrochemical window of 1.5–4.0 V at different scan rates. (B) Cycling response of interconnected $K_{0.7}Fe_{0.5}Mn_{0.5}O_2$ nanowires analyzed by the Randles-Sevick equation. (C) CV curves of $K_{0.7}Fe_{0.5}Mn_{0.5}O_2$ particles in the electrochemical window of 1.5–4.0 V at different scan rates. (D) Cycling response of $K_{0.7}Fe_{0.5}Mn_{0.5}O_2$ particles analyzed by the Randles-Sevick Equation.

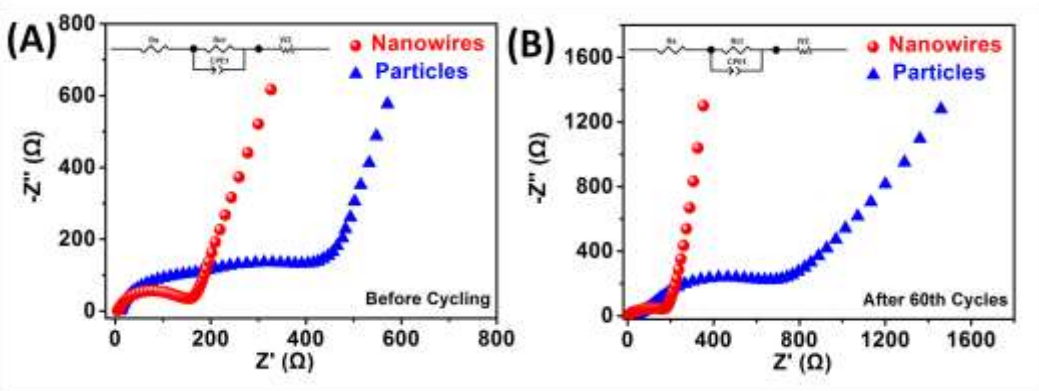

Figure S11. (A) AC impedance plots of interconnected $K_{0.7}Fe_{0.5}Mn_{0.5}O_2$ nanowires and $K_{0.7}Fe_{0.5}Mn_{0.5}O_2$ particles before cycling (from 0.1Hz to 100 kHz). (B) AC impedance plots of interconnected $K_{0.7}Fe_{0.5}Mn_{0.5}O_2$ nanowires and $K_{0.7}Fe_{0.5}Mn_{0.5}O_2$ particles after 60 cycles at 100 mA g^{-1} (from 0.1Hz to 100 kHz).

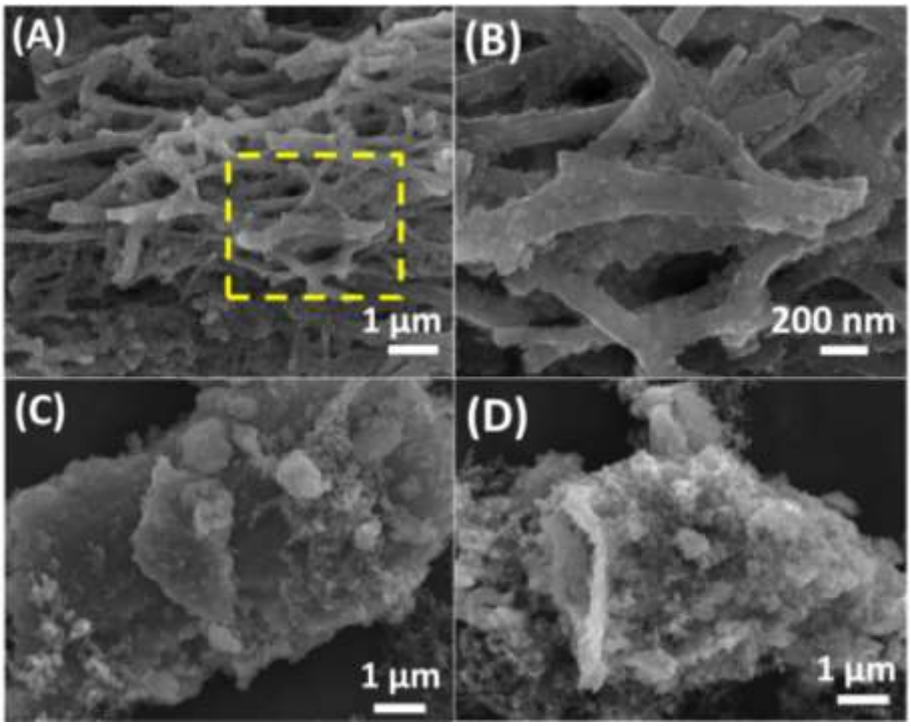

Figure S12. (A, B) SEM images of interconnected $K_{0.7}Fe_{0.5}Mn_{0.5}O_2$ nanowires after 60 cycles at 100 mA g^{-1} in K-ion batteries. (C, D) SEM images of $K_{0.7}Fe_{0.5}Mn_{0.5}O_2$ particles after 60 cycles at 100 mA g^{-1} in K-ion batteries.

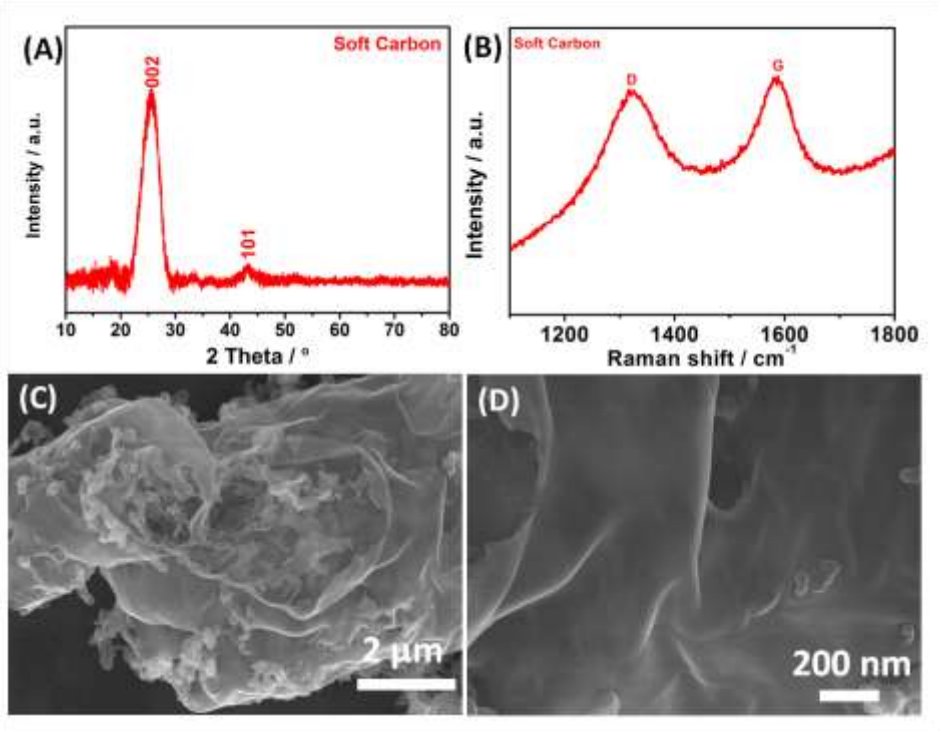

Figure S13. XRD pattern (A) and Raman spectra (B) of soft carbon sintered at 900 °C in argon for 10h. (C, D) SEM images of soft carbon.

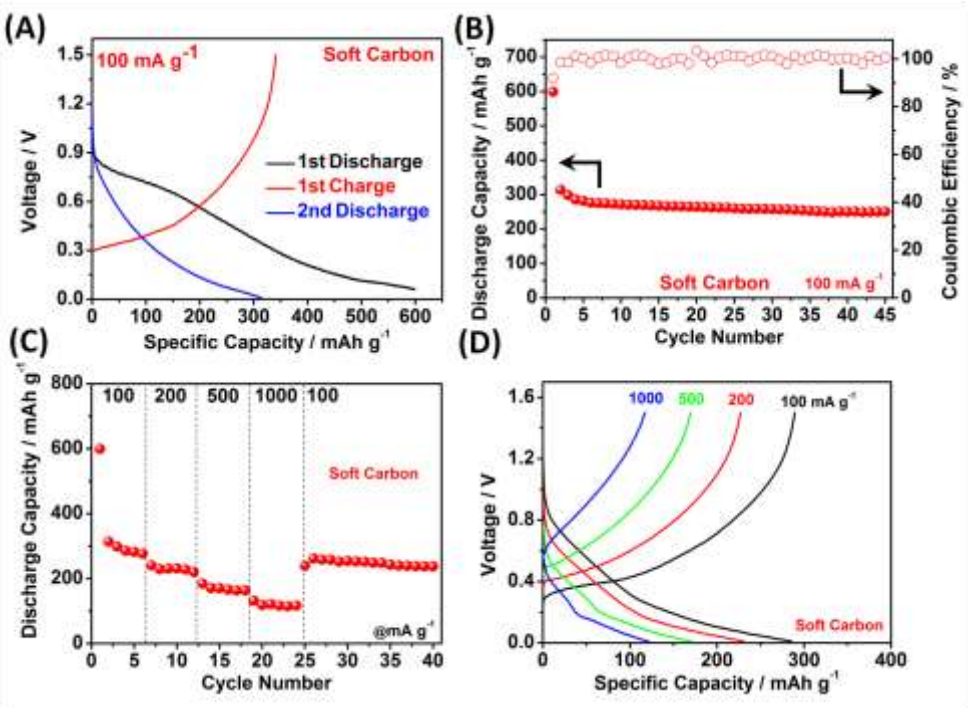

Figure S14. Electrochemical performances of soft carbon. (A) Charge/discharge curves of soft carbon in the electrochemical window of 1.5–4.0 V at 100 mA g^{-1}. (B) Cyclic performance and the corresponding Coulombic efficiency of soft carbon at 100 mA g^{-1}. (C) Rate performance of soft carbon at various rates ranging from 100, 200, 500, 1000 and return to 100 mA g^{-1}. (D) Charge/discharge curves of soft carbon at various current densities.

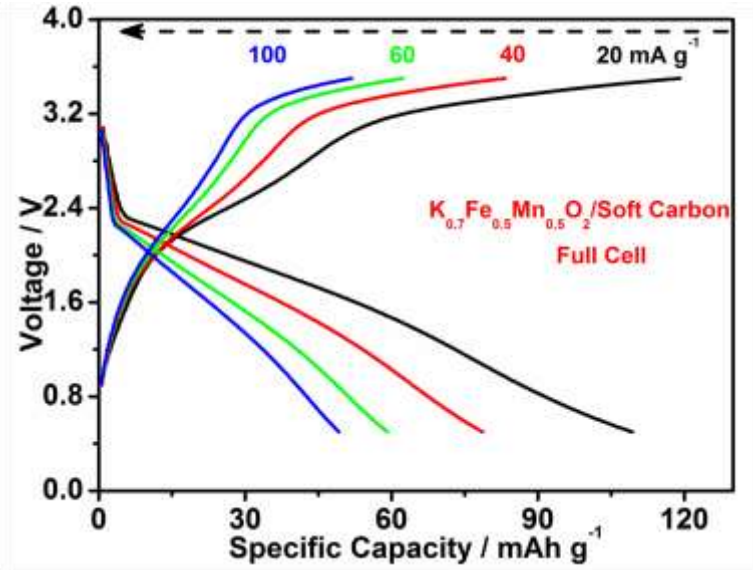

Figure S15. Charge/discharge curves of the full cell at various current densities in K-ion full batteries.

Table S2. Comparison of the electrochemical performances of some cathode materials in K-ion batteries or K-ion full batteries.

Active materials	Voltage ranges (V)	Current density (mA g^{-1})	Initial capacity (mAh g^{-1})	Cycle numbers	Capacity retention	System
Interconnected $K_{0.7}Fe_{0.5}Mn_{0.5}O_2$ Nanowires Half Cells (This Work)	1.5–4.0	20	178	45	70%	Non-aqueous
		100	114	60	89%	
		200	94	45	94%	
		500	79	200	85%	
		1000	68	450	87%	
Nickel Hexacyanoferrate Nanoparticle Half Cells[14]	0.3–1.0	500	50	1000	98.25%	Aqueous
Prussian Green ($KFe^{III}Fe^{II}(CN)_6$) Half Cells[16]	0–1.0	111	140	20	87.9%	Aqueous
3,4,9,10-perylene-tetracarboxylicacid-dianhydride(PTCDA) Half Cells[17]	1.5–3.5	10	130	200	70%	Non-aqueous
$K_2C_6O_6$ Half Cells[26]	1.0–3.2	40	212	–	–	Non-aqueous
		1000	171	–	–	
Interconnected $K_{0.7}Fe_{0.5}Mn_{0.5}O_2$ Nanowires/Soft Carbon Full Cells (This Work)	0.5–3.5	40	82	50	75%	Non-aqueous
		100	50	100/250	85%/76%	
$K_2C_6O_6/K_4C_6O_6$ Full Cells[26]	0.5–2.0	25	75	10	60%	Non-aqueous